Original Article

Diffusion kurtosis and intravoxel incoherent motion in predicting postpartum hemorrhage in patients at high risk for placenta accreta spectrum disorders

Tao Lu[#], Mou Li[#], Hang Li, Yishuang Wang, Xinyi Zhao, Yan Zhao, Na Wang

Department of Radiology, Sichuan Provincial People's Hospital, University of Electronic Science and Technology of China, Chengdu, China

Contributions: (I) Conception and design: T Lu, Y Zhao; (II) Administrative support: T Lu, N Wang; (III) Provision of study materials or patients: Y Wang, M Li; (IV) Collection and assembly of data: M Li, H Li; (V) Data analysis and interpretation: M Li, X Zhao; (VI) Manuscript writing: All authors; (VII) Final approval of manuscript: All authors.

[#]These authors contributed equally to this work.

Correspondence to: Tao Lu, MD. Department of Radiology, Sichuan Provincial People's Hospital, University of Electronic Science and Technology of China, 32 West Second Section, First Ring Road, Chengdu 610072, China. Email: 345248302@qq.com; elisa.lulu@gmail.com.

Background: Placenta accreta spectrum (PAS) disorder encompasses a spectrum of pathologies, from placenta accreta to placenta percreta, which is usually associated with postpartum hemorrhage (PPH).

Methods: This cross-sectional study enrolled 109 patients suspected of having PAS disorders based on previous ultrasound results or clinical risk factors from November 2018 to March 2022 in Sichuan Provincial People's Hospital. Of the 109 patients, 34 had PPH and 75 did not have PPH. Magnetic resonance imaging (MRI) including diffusion-weighted imaging (DWI), intravoxel incoherent motion (IVIM), and diffusion kurtosis imaging (DKI) was performed for each patient and the apparent diffusion coefficient (ADC) from DWI, perfusion fraction (f), pure diffusion coefficient (D), and pseudo-diffusion coefficient (D*) from IVIM, and mean diffusion kurtosis (MK) and mean diffusion coefficient (MD) from DKI were measured and compared. The correlation between the DWI parameters and estimated blood loss (EBL) during surgery was identified using correlation analysis. The diagnostic performance for predicting PPH was compared between the two methods.

Results: The amount of bleeding during delivery was positively correlated with D [r=0.331, P<0.001, 95% confidence interval (CI): 0.170 to 0.477], D* (r=0.389, P<0.001, 95% CI: 0.207 to 0.527), f (r=0.222, P=0.02, 95% CI: 0.036 to 0.398), and MD (r=0.277, P=0.003, 95% CI: 0.108 to 0.439), but negatively correlated with MK (r=–0.280, P=0.003, 95% CI: –0.431 to –0.098). In predicting PPH, multivariate analyses showed the independent risk factors were placenta previa and D; the area under the curve (AUC) was 0.795 (95% CI: 0.711 to 0.878) when the two risk factors were combined together.

Conclusions: IVIM and DKI parameters are correlated with EBL. The combined use of placenta previa and D are helpful for predicting PPH in patients at high risk of PAS disorders.

Keywords: Placenta accreta spectrum disorders; diffusion-weighted MRI; intravoxel incoherent motion (IVIM); diffusion kurtosis imaging (DKI)

Submitted Sep 14, 2022. Accepted for publication Jul 19, 2023. Published online Aug 08, 2023.
doi: 10.21037/qims-22-966
View this article at: https://dx.doi.org/10.21037/qims-22-966

Introduction

Placenta accreta spectrum (PAS) disorders represent an abnormal condition involving placental trophoblastic attachment to or invasion of the myometrium due to a defect of the deciduas comprising placenta accreta, increta, and percreta. The prevalence of PAS disorders was reported to be 1 in 540–2,500 deliveries in western counties due to the increased number of uterine interventions, especially cesarean deliveries (CD) (1). The incidence of PAS disorders was 1 in 506 from 1990 to 2007 in China, which increased to 1 in 42 from 2013 to 2015 (2,3), along with the increased CD rates. Besides CD, placenta previa, advanced maternal age, use of assisted reproductive technologies, and uterine surgeries have all been identified as risk factors for PAS disorders (4).

PAS is commonly associated with postpartum hemorrhage (PPH) and its secondary complications include multisystem organ failure, disseminated intravascular coagulation, intensive care unit (ICU) admission, hysterectomy, and even death when manually removing the placenta, and thus is correlated with high maternal morbidity and mortality (5-10).

It has been suggested that maternal morbidity and blood loss are reduced in cases of prenatal planned CD rather than emergency CD (11-13). Prenatal prediction of PPH will allow appropriate treatment options and planned preterm delivery, which facilitate preoperative consultation and improve patient prognosis (14-16).

Ultrasonography (US) is recommended as the primary modality in antenatal diagnosis of PAS, yet the use of magnetic resonance imaging (MRI) has continued to rise, especially in tertiary centers. Besides, US does not provide sufficient quantitative parameters in evaluating the placenta. A recent functional MRI may provide information about placental function. Diffusion-weighted imaging (DWI) is a non-invasive MRI technique that provides microstructural and physiological information about tissues. Intravoxel incoherent motion (IVIM) is a bi-exponential DWI model which aims to quantify perfusion and diffusion of the tissue. Diffusion kurtosis imaging (DKI) is another DWI model utilized in the quantification of the heterogeneity and cellularity of the tissue (17). Our previous studies employed these two DWI models to explore placental function in patients with PAS disorders; the ability of DWI parameters to predict PPH has not yet been ascertained (18,19).

The first aim of this study was to investigate the correlation between these different DWI parameters and the amount of intraoperative bleeding. The second aim was to investigate whether IVIM and DKI parameters could be applied to predict PPH. We present this article in accordance with the STROBE reporting checklist (available at https://qims.amegroups.com/article/view/10.21037/qims-22-966/rc).

Methods

This cross-sectional study was conducted in accordance with the Declaration of Helsinki (as revised in 2013). The study was approved by the institutional review board (IRB) of Sichuan Provincial People's Hospital and written informed consent was provided by each female participant. A total of 198 patients underwent placental MRI with a DWI sequence between November 2018 and March 2022. The inclusion criteria were as follows: (I) patients with singleton pregnancy and suspected of having a PAS disorder; and (II) fetal development coinciding with gestational age (GA). The exclusion criteria were as follows: (I) pre-existing renal disease, diabetes mellitus, and chronic hypertension; (II) unavailability of medical records; (III) suspected placental insufficiency; and (IV) patients with severe motion artifacts or poor image quality. Finally, 109 patients (mean age 31.33±4.56 years, range 22–45 years), mean gestational GA at 31 weeks (range, 16–38 weeks) were enrolled (*Figure 1*). We calculated sample size using MedCalc software (MedCalc Software, Ostend, Belgium) for the purpose of estimating of different diagnostic accuracies. The sample size included in this study was greater than the estimated sample size.

Clinical characteristic analysis

Clinical indicators for PAS disorders were collected including maternal age, gravidity, parturition, abortions, previous CD, GA at examination, GA at delivery, amount of bleeding during surgery, and transfusion protocol.

MRI protocols

MRI examinations were conducted at 1.5T scanner (Aera; Siemens Healthineers, Erlangen, Germany) using a phase-array body matrix coil. The MRI protocol included the following sequences: half Fourier acquisition single-shot turbo spin-echo (HASTE), true fast imaging with steady-state precession (TrueFISP), T1-weighted imaging T1WI, and DWI. DWI was acquired using a single-shot echo-planar imaging (EPI) sequence under free breathing. A total

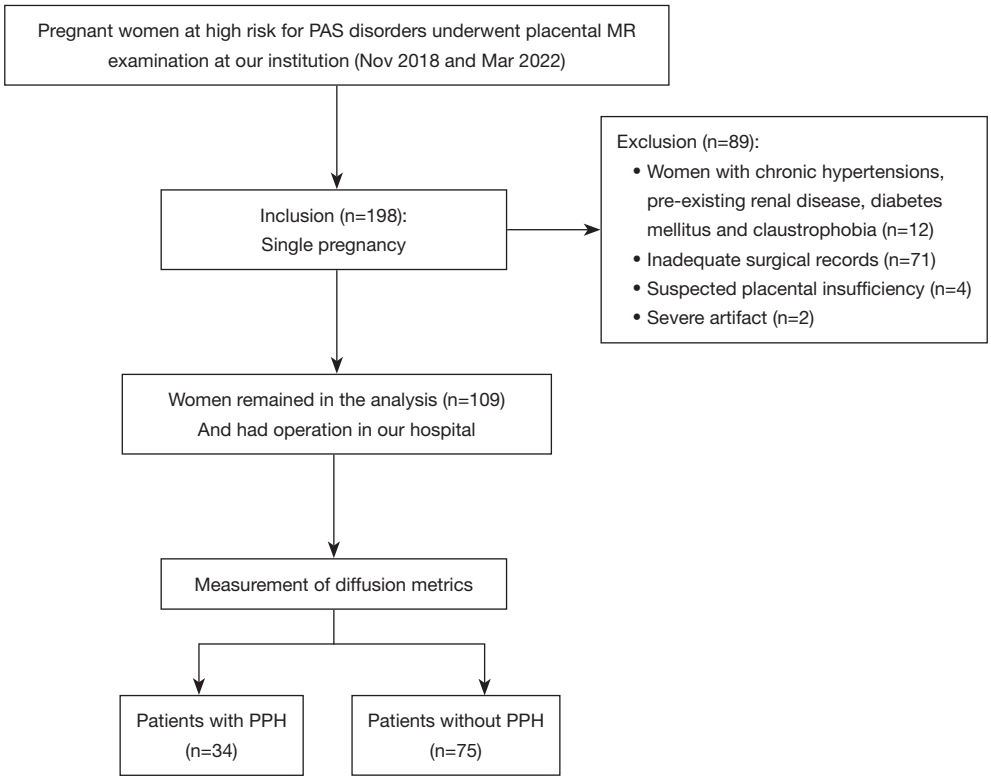

Figure 1 Flowchart of the study design. PAS, placenta accreta spectrum; MR, magnetic resonance; PPH, postpartum hemorrhage.

of 11 b-values (0, 50, 100, 150, 200, 400, 600, 800, 1,000, 1,200, and 1,600 s/mm^2) with a number of averages of 2 in 3 orthogonal directions was used. The scanning parameters were as follows: repetition time/echo time (TR/TE) =5,200/83 ms, matrix size =192×120, field of view (FOV) =390 mm, slice thickness =5 mm, intersection gap =5 mm, and parallel imaging acceleration factor =2. The total scan time was 7 minutes 29 seconds.

Image processing and analysis

Post-processing of the DWI data was performed with a research software IMAgenGINE (Vision Technologies Ltd., Burnie, MD, USA) to obtain DWI parameters (20). Mean diffusion coefficient (MD) and mean diffusion kurtosis (MK) were calculated based on the following formula using 6 b-values (b=0, 400, 800, 1,000, 1,200, and 1,600 s/mm^2) (21,22): $Sb/S0 = \exp(-b \times MD + b^2 \cdot MD^2 \times MK/6)$. Sb and S0 are the signal intensities acquired with the diffusion gradient factors of b and 0, respectively.

IVIM parameters calculation was performed by following the formula using 8 b-values (b= 0, 50, 100, 150, 200, 400, 600, 800 s/mm^2) (23,24): $Sb/S0 = (1-f) \exp(-b \times D) + f \exp(-b \times (D + D^*))$, wherein f is the perfusion fraction, D is the diffusion coefficient, and D* is the pseudo-diffusion coefficient.

The apparent diffusion coefficient (ADC) was calculated following the standard monoexponential fit with b-values of 0 and 1,000 s/mm^2: $Sb/S0 = \exp(-b \times ADC)$.

The measurements were conducted separately by two independent radiologists with 5 and 8 years of experience in obstetric imaging, respectively. The two readers were blind to the patient grouping information. Regions of interest (ROIs) were drawn along the entire margin of the placenta on each DWI slice with b=0 s/mm^2 (*Figure 2*). To avoid partial volume effects, the size of ROIs was slightly smaller than the placental margin to calculate ADC, MD, MK, D, D*, and f values, and then the diffusion parameter maps were produced.

Reference standard

The estimated blood loss (EBL) was measured from blood volumes in sponges and suction containers in the operating

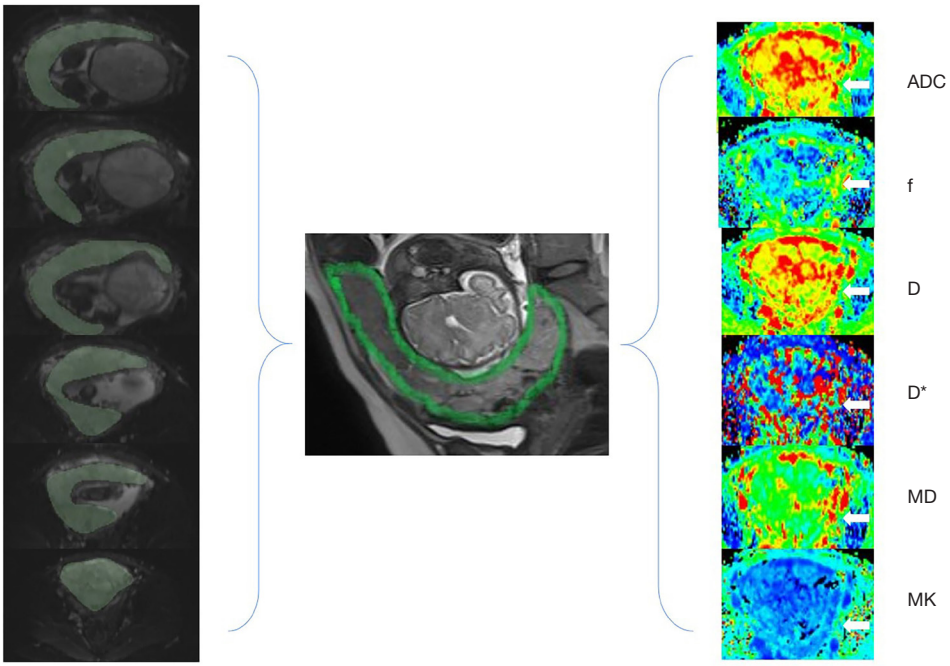

Figure 2 The schematic illustration of ROIs of the placenta. The ROIs were drawn covering the whole placenta and the diffusion parameter maps were automatically produced (arrow). The green circle indicates the margin of the placenta. ADC, apparent diffusion coefficient; f, perfusion fraction; D, pure diffusion coefficient; D*, pseudo-diffusion coefficient; MD, mean diffusion coefficient; MK, mean diffusion kurtosis; ROIs, regions of interest.

room; non-quantifiable blood loss was visually estimated. PPH was defined as intrapartum/peripartum blood loss of >1,000 mL.

Statistical analysis

Quantitative variables that followed a normal distribution were presented as mean ± standard deviation (SD), variables following a nonnormal distribution were presented as median (quartile), and categorical variables were presented as numbers (proportions, %). The correlation between DWI parameters and EBL during surgery was analyzed by correlation analysis.

Mann-Whitney *U*-test and χ^2 test were used for the comparisons of clinical characteristics in patients with and without PPH. As the DWI parameters followed a nonnormal distribution, comparisons of the DWI parameters between patients with and without PPH were made with the Mann-Whitney *U*-test. A multivariate logistic regression analysis was used to determine the most significant risk factors in predicting PPH. Receiver operating characteristic (ROC) curve analyses were performed to evaluate the diagnostic performance of significant parameters.

The inter- and intra-reader agreement of DKI and IVIM parameters was assessed by using the intraclass correlation coefficient (ICC) with 95% confidence intervals (CI). Statistical significance was considered when a 2-sided P value was <0.05. Statistical analyses were performed with SPSS 21.0 (IBM Corp., Armonk, NY, USA).

Results

In our patients, previous uterine dilation and curettage (n=83), placenta previa (n=81), age ≥35 years (n=27), multiparity (n=11), previous CD (n=7), uterine myoma surgery (n=2), in vitro fertilization (IVF) procedure (n=1), and uterine anomaly (n=1) were all identified as risk factors for PAS disorders.

Maternal characteristics of the study participants are summarized in *Table 1*. Of the total 109 participants, 34 (31.19%) had PPH; among those without PPH, 60 (80%) underwent a planned CD, whereas among the patients with PPH, all (100%) underwent a planned CD. Among the patients with PPH, 16 received abdominal artery balloon occlusion, 19 underwent ligation of the uterine artery,

Table 1 Maternal characteristics in the study groups

Parameters	Patients without PPH (N=75)	Patients with PPH (N=34)	P value
Age (years)	30.57±4.11	33.03±5.09	0.32
Less than 35	62 (82.66)	20 (66.15)	0.008
35 or older	13 (17.33)	14 (33.85)	
Gestational age at examination (weeks)	31 [5]	30.5 [4]	0.366
Gestational age at the time of delivery (weeks)	37 [2]	36 [3]	0.001
Previous caesarean section			0.07
Yes	44 (58.67)	26 (76.47)	
No	31 (41.33)	8 (23.53)	
Number of previous caesarean section			0.22
0	32 (42.67)	9 (26.47)	
1	37 (49.33)	20 (58.82)	
2 or more	6 (8.00)	5 (14.71)	
Previous uterine dilation and curettage			0.01
Yes	52 (69.33)	31 (91.18)	
No	23 (30.67)	3 (8.82)	
Number of previous uterine dilation and curettage			0.05
0	22 (29.33)	2 (5.88)	
1	18 (24.00)	13 (38.24)	
2 or more	35 (46.67)	19 (55.88)	
Placenta previa			<0.001
Yes	47 (62.67)	34 (100.00)	
No	28 (37.33)	0 (0.00)	

Data are represented as number (%) or mean ± standard deviation or median [quartile]. PPH, postpartum hemorrhage.

4 received uterine balloon tamponade, and 3 patients underwent hysterectomy. Patients with PPH were more likely to be older than 35 years (P=0.008), and were more likely to deliver earlier, have more previous uterine dilations and curettages, and have placenta previa (P=0.001, P=0.05, and P<0.001, respectively).

The agreement of the DWI parameters was excellent for the volumetric analysis of the placenta (*Table 2*).

D (r=0.331, P<0.001, 95% CI: 0.170 to 0.477), D* (r=0.389, P<0.001, 95% CI: 0.207 to 0.527), f (r=0.222, P=0.02, 95% CI: 0.036 to 0.398), and MD (r=0.277, P=0.003, 95% CI: 0.108 to 0.439) were positively correlated with EBL, whereas MK (r=–0.280, P=0.003, 95% CI: –0.431 to –0.098) was negatively correlated with it (*Figure 3*).

Comparisons of DWI parameter showed that D and D* were significantly higher (P=0.003 and P=0.001, respectively) whereas MK was significantly lower in patients with PPH (P=0.006) (*Table 3*, *Figures 4*,*5*). For predicting PPH, D* demonstrated the highest AUC of 0.706 (95% CI: 0.6 to 0.812), followed by placenta previa of 0.687 (95% CI: 0.589 to 0.784) and D of 0.681 (95% CI: 0.574–0.778). Multivariate logistic regression analysis showed that placenta previa and D differed significantly between patients with and without PPH (P=0.002 and P=0.01, respectively) (*Table 4*). We further combined placenta previa and D to predict PPH. The combination of the two risk factors showed the best overall performance, showing the highest sensitivity of 65%, specificity of 81%, and AUC of 0.795 (*Figure 6*). The diagnostic performances of parameters including placenta previa, D, D*, MK, and the combination

Table 2 The inter-reader and intra-reader reproducibility for DWI parameters

Parameters	ICC (95% CI)	
	Inter-reader	Intra-reader
Standard DWI parameters		
ADC mean ($\times10^{-3}$ mm^2/s)	0.822 (0.713–0.892)	0.948 (0.902–0.972)
DKI parameters		
MD mean ($\times10^{-3}$ mm^2/s)	0.737 (0.589–0.838)	0.818 (0.678–0.901)
MK mean	0.911 (0.853–0.947)	0.947 (0.901–0.972)
IVIM parameters		
f mean (%)	0.715 (0.557–0.823)	0.804 (0.654–0.893)
D mean ($\times10^{-3}$ mm^2/s)	0.872 (0.770–0.927)	0.937 (0.881–0.967)
D* mean ($\times10^{-3}$ mm^2/s)	0.666 (0.470–0.795)	0.652 (0.426–0.802)

DWI, diffusion-weighted imaging; ICC, intraclass correlation coefficient; CI, confidence interval; ADC, apparent diffusion coefficient; DKI, diffusion kurtosis imaging; MD, mean diffusion coefficient; MK, mean diffusion kurtosis; IVIM, intravoxel incoherent motion; f, perfusion fraction; D, pure diffusion coefficient; D*, pseudo-diffusion coefficient.

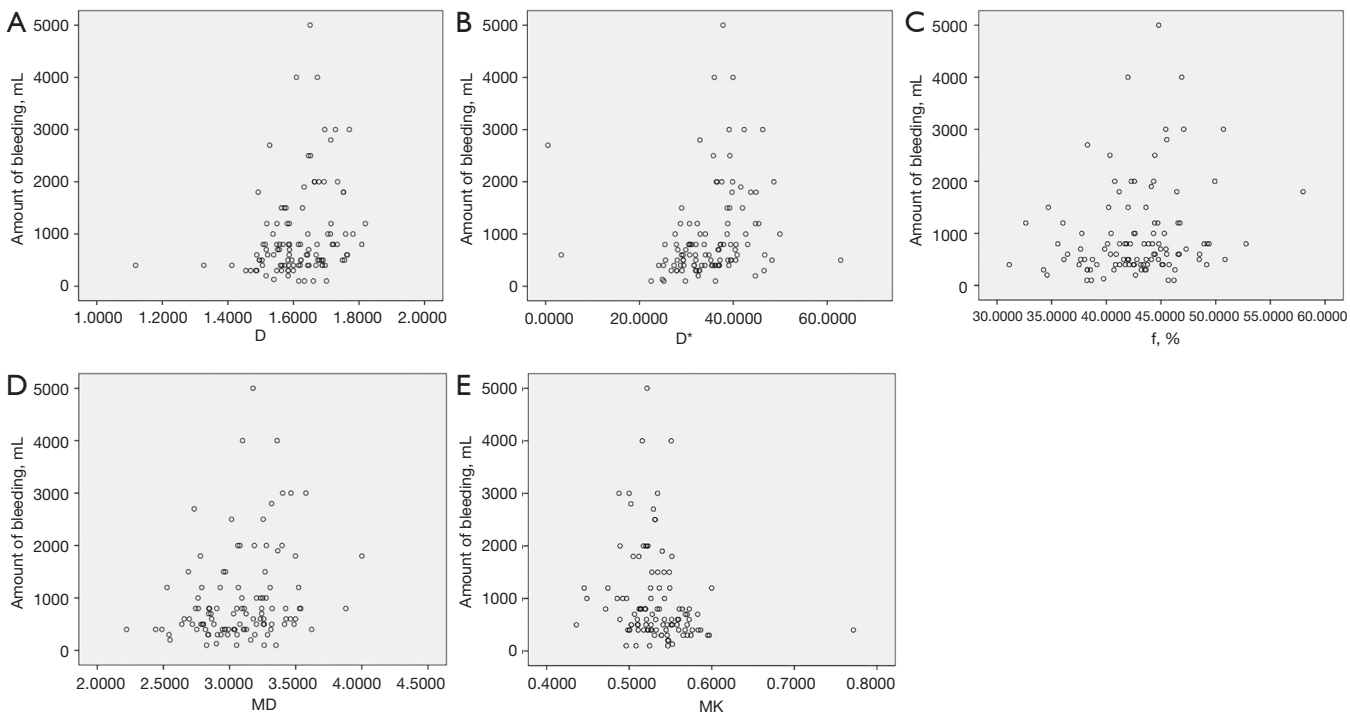

Figure 3 Scatter plots of DWI parameters and the amount of bleeding. The scatter plots showed that D, D*, f, and MD were positively correlated with EBL (A-D), MK was negatively correlated with EBL (E). D, pure diffusion coefficient; D*, pseudo-diffusion coefficient; f, perfusion fraction; MD, mean diffusion coefficient; MK, mean diffusion kurtosis; DWI, diffusion-weighted imaging; EBL, estimated blood loss.

Table 3 Comparison of DWI parameters between patients with and without PPH (n=109)

Parameters	Patients without PPH	Patients with PPH	P value
Standard DWI parameters			
ADC mean ($\times10^{-3}$ mm^2/s)	1.528 (0.104)	1.544 (0.092)	0.19
DKI parameters			
MD mean ($\times10^{-3}$ mm^2/s)	3.039 (0.417)	3.195 (0.363)	0.09
MK mean	0.536 (0.453)	0.5212 (0.035)	0.006
IVIM parameters			
f mean (%)	42.667 (5.242)	43.970 (5.076)	0.66
D mean ($\times10^{-3}$ mm^2/s)	1.588 (0.128)	1.664 (0.137)	0.003
D* mean ($\times10^{-3}$ mm^2/s)	32.517 (8.152)	38.759 (8.634)	0.001

Data are shown as median (quartile). DWI, diffusion-weighted imaging; PPH, postpartum hemorrhage; ADC, apparent diffusion coefficient; DKI, diffusion kurtosis imaging; MD, mean diffusion coefficient; MK, mean diffusion kurtosis; IVIM, intravoxel incoherent motion; f, perfusion fraction; D, pure diffusion coefficient; D*, pseudo-diffusion coefficient.

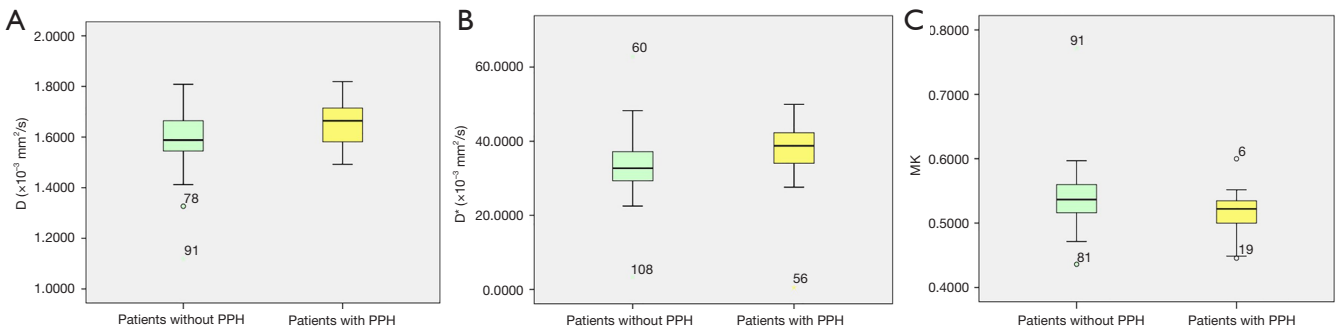

Figure 4 Box and whisker plots of different DWI parameters. (A) D was significantly higher in patients with PPH. (B) D* was significantly higher in patients with PPH. (C) MK was significantly lower in patients with PPH. D, pure diffusion coefficient; D*, pseudo-diffusion coefficient; MK, mean diffusion kurtosis; PPH, postpartum hemorrhage.

of placenta previa and D for PPH prediction are detailed in *Table 5*.

Discussion

Our study showed positive correlations between D, D*, f, and MD and EBL during surgery, and a negative correlation between MK and EBL. In PAS, larger radial and arcuate arteries deep in the myometrium were infiltrated by invasive extravillous trophoblasts, leading to loss of muscular elastic tissue from their walls and vessel enlargement (25,26). Thus, massive hemorrhage occurs as these larger arteries conduct a far larger blood volume when removing the invasive placenta. The f represents the moving blood volume fraction compared with total voxel volume, D* reflects the intervillous spaces and fetal capillaries blood movement, and D reflects cellular and interstitial characteristics of the tissue in placental IVIM (27,28). The positive correlation between the three IVIM parameters and EBL suggests that the placenta is increasingly hypervascular with increased microcirculatory perfusion in the capillary network and increased diffusion motion of pure water molecules when the amount of bleeding increases.

DKI is a non-Gaussian DWI model depicting non-Gaussian water movement with higher b values. DKI has been mainly adopted in tumors to quantify tissue heterogeneity and cellularity (21-24). MD is the corrected ADC for non-Gaussian bias and has a similar change to D as they are both diffusion-related coefficients. Therefore, MD is also positively correlated with EBL. In general terms, MK

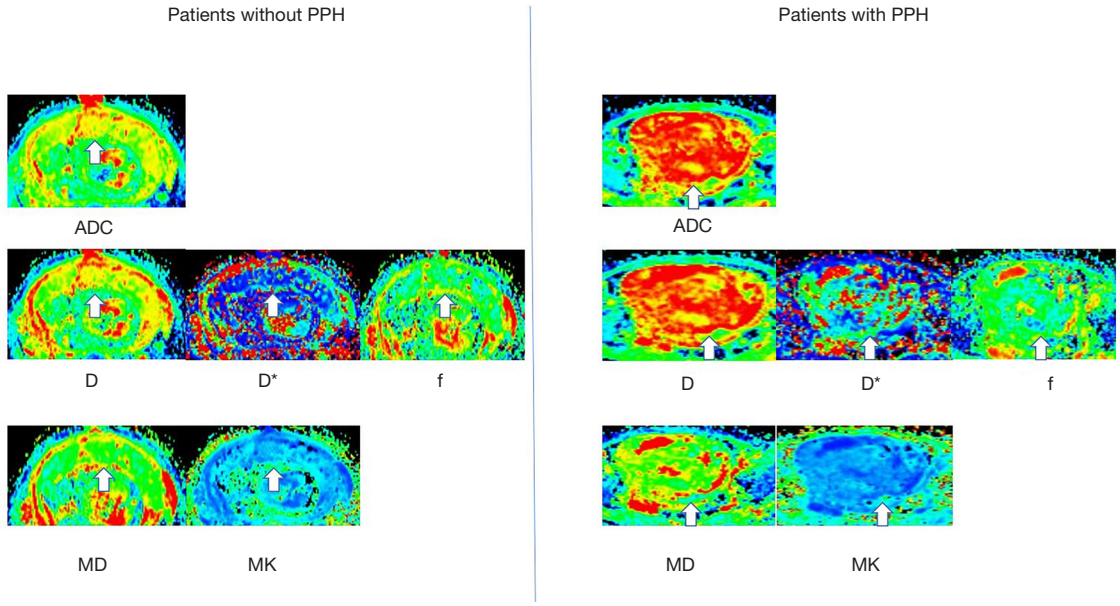

Figure 5 The illustration of DWI parameters in patients with and without PPH. The figure shows a 36-year-old woman with PPH and a 27-year-old woman without PPH. The former had placenta previa and 1 prior CD and the latter had 1 prior CD only. The figure demonstrates heterogeneous hyperintensity on ADC, D, D*, and MD map, and hypointensity on MK map (arrow). PPH, postpartum hemorrhage; ADC, apparent diffusion coefficient; D, pure diffusion coefficient; D*, pseudo-diffusion coefficient; f, perfusion fraction; MD, mean diffusion coefficient; MK, mean diffusion kurtosis; DWI, diffusion-weighted imaging; CD, cesarean delivery.

Table 4 Multivariate logistic regression analysis of risk factors for patients with PPH

Variables	Multivariate analysis	
	OR (95% CI)	P value
Placenta previa		0.002
No	1	
Yes	1.723 (1.432–2.074)	
D	15.085 (5.841–38.954)	0.01

PPH, postpartum hemorrhage; D, pure diffusion coefficient; OR, odds ratio; CI confidence interval.

is altered by tissue complexity or cellular heterogeneity and measures the deviation of tissue water molecules' diffusion from a Gaussian distribution (29). The moving blood may compromise the deviation of diffusion distribution from Gaussian form, thus resulting in the negative correlation between MK and EBL.

Our study also showed that D and D* were significantly

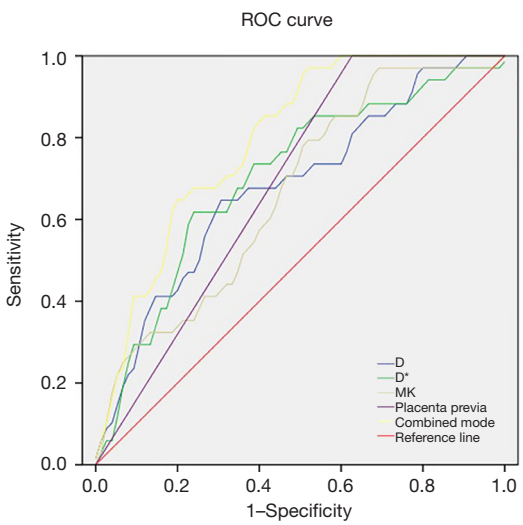

Figure 6 ROC curves for predicting patients with PPH. The combination of placenta previa and D showed the best overall performance. D, pure diffusion coefficient; D*, pseudo-diffusion coefficient; MK, mean diffusion kurtosis; ROC, receiver operating characteristic; PPH, postpartum hemorrhage.

Table 5 Predictive performance of risk factors for patients with PPH

Risk factors	AUC	Accuracy (%)	Sensitivity (%)	Specificity (%)	PPV (%)	NPV (%)
Placenta previa	0.687	68.7	100	37.3	61.46	100.00
D	0.681	68.0	65	71.0	69.15	66.98
D*	0.706	69.5	62	77.0	72.94	66.96
MK	0.664	64.0	49	79.0	70.00	60.77
Combination of placenta previa and D	0.795	73.0	65	81.0	77.38	69.83

PPH, postpartum hemorrhage; AUC, area under the curve; PPV, positive predictive value; NPV, negative predictive value; D, pure diffusion coefficient; D*, pseudo-diffusion coefficient; MK, mean diffusion kurtosis.

higher and MK was significantly lower in patients with PPH, whereas f and MD did not differ between patients with and without PPH. The results demonstrated the increased diffusion motion of water molecules in the extracellular spaces and increased motion of blood water molecules in the capillary network, with decreased cellular vheterogeneity in patients with PPH. In patients with higher risks of PAS disorders, preferential attachment of the blastocyst to scar tissue facilitates abnormally deep invasion of trophoblastic cells and subsequent neovascularization or dilation of the myometrial vasculature (30). These events possibly result in increased blood movement in the fetal capillaries and increased diffusion motion of extravascular water molecules within the placental villi in patients with PPH. The parameter f represents the relative amount of blood flowing through the vascular bed (31). Previous studies have reported decreased f values in fetal growth restriction (FGR) pregnancies, maternal vascular malperfusion, and those delivering small for GA (SGA) neonates (32-35). As PAS disorders are not a vascular disease of the placenta, the microvascular perfusion was similar in patients with and without PPH.

DKI was introduced to describe water diffusion deviating from the Gaussian law due to microenvironment complexity, such as macromolecules, cell membranes, or vessels (36). In tumors, DKI is usually used to reflect structural heterogeneity of different tumors with varying degrees of cellularity. However, the application and interpretation of DKI in the placenta has not been delineated. MD is the corrected diffusion coefficient, which is related to the Gaussian behavior and similar to ADC. It is influenced by both perfusion and diffusion information within the tissue. Therefore, both MD and ADC did not differ in placentas in patients with and without PPH, as MD showed similar behavior to ADC. MK is considered to represent the direct interaction between water molecules and intracellular compounds and cell membrane (37). As motion of blood water molecules in the capillary network increased in patients with PPH, the membrane permeability also increased, resulting in decreased MK value.

Massive obstetric hemorrhage remains a leading cause of maternal death. As it is potentially avoidable, antenatal prediction of PPH with imaging modalities is pivotal in patients at high risk for PAS. Patients carrying a high probability of PPH will require the care of a dedicated multidisciplinary team and an appropriate delivery schedule, thus patients' clinical outcome can be significantly improved (38). Chen *et al.* developed a risk prediction model for severe PPH based on clinical and ultrasound imaging information in patients with placenta previa; the sensitivity, specificity, and AUC were 76.5%, 90%, and 0.84, respectively (39). Lee *et al.* established a scoring model including clinical and ultrasound signs to predict PPH in patients with placenta previa; the sensitivity, specificity, and AUC were 81%, 77%, and 0.856, respectively (40). The above studies claimed that the risk prediction model or scoring model might be useful for predicting massive PPH. However, using ultrasound images lacks an objective evaluation standard, and the diagnostic accuracy depends on the experience of the operator. In recent years, there has been growing interest in the use of MRI features for evaluating the placenta (41). It should be acknowledged that interpreting MRI images also requires professional training, with experienced radiologists having demonstrated higher accuracy in diagnosing PAS (42).

Our study showed that placenta previa and D are independent risk factors for predicting PPH. We further combined placenta previa and D for predicting PPH. The sensitivity, specificity, positive predictive value (PPV), and negative predictive value (NPV) were 77.38%, 69.83%,

65%, and 81%, respectively, with an AUC of 0.795. Placenta previa and D together performed better than any of placenta previa and D, D*, and MK individually. Therefore, the combination of placenta previa and D could be used to identify patients who are likely to have PPH. These patients then can be managed with careful delivery planning including requiring blood transfusion, and ICU admission by specialized surgical teams, thus maternal mortality and morbidity can be reduced. Although the diagnostic performance of our model in predicting PPH was lower than that of previous ultrasound studies, the quantitative assessment of the placenta using DWI parameters is needed for objective evaluation. The ROI delineation of our study covered the entire placental slices, which did not rely on the experience of the radiologists. The good inter-observer agreement also confirmed the reliability of the measurements. Our model avoided the subjective evaluation of MRI images and thus can be an effective tool to predict PPH in clinical practice.

The first limitation of our study is the small number of patients, which led to inevitable selection bias. Only 34 patients with PPH were enrolled in this study. The correlation between DWI parameters and blood loss was low. Further studies with more patients, especially those with PPH, are essential to determine the correlation between DWI parameters and blood loss regardless of the different surgical techniques used. Second, there are inherent difficulties regarding estimation of blood loss during surgery. The current method of EBL may show unreliability among surgeons and institutions; however, there has been no recommended method in the guidelines, and the visual estimate and weighing methods are more common in clinical use. Third, as placenta previa is a most common risk factor of PAS, it had an NPV of 100% for PPH which undermined the findings of this study. However, other PAS risk factors also include previous CD, advanced maternal age, previous uterine surgery, assisted reproductive technology, and other uterine abnormalities. Our results may be applied to patients with risk factors for PAS other than placenta previa. We also believe future studies regarding the prediction of PPH in patients with placenta previa is essential. Fourth, histopathology was lacking in this study. Histopathological findings are essential in many medical conditions as they provide gold standards for the definition. However, clinical description is the most important criteria for definition and stratification of PAS, as some cases involved manual removal of the placenta during CD and pathological specimens were not submitted. Fifth, in this study, a free-breathing protocol was utilized, as obtaining breath-hold images from pregnant women is usually impossible. This protocol may lead to a decreased signal-to-noise ratio (SNR) on parameter maps. However, the excellent interreader agreement in our study confirmed the reliability of the measurements. Sixth, DKI is very sensitive to microstructural complexity of tissues at high b values. However, T2 relaxation accelerates at high b values leading to a reduced SNR. Considering the relatively low SNR resulting from the use of high b values, 1,600 s/mm^2 was set as the maximum b value in this study, smaller than the recommended 2,000 s/mm^2 for other abdominal organs with DKI (22,23,43). Overall, we think that the b values settings was adequate for this study as this protocol shows satisfactory imaging quality, supporting the present results. Seventh, we acknowledged that MRI is not a prenatal screening tool currently, the cost and availability of MRI may be limiting factors for its utilization relative to US.

Conclusions

In conclusion, IVIM and DKI parameters were correlated with EBL in patients at high risk for PAS disorders. D and D* were significantly higher and MK was significantly lower in patients with PPH. A combination of placenta previa and D are useful for predicting PPH. The results of our study would help in early prediction of PPH and thus facilitate the management of subsequent patients. Future study with larger sample size and focusing on patients with placenta previa are needed to explore the relationship between DWI parameters and patient outcomes.

Acknowledgments

Funding: This research was supported by Sichuan Province Science and Technology Program (No. 2021YJ0237).

Footnote

Reporting Checklist: The authors have completed the STROBE reporting checklist. Available at https://qims.amegroups.com/article/view/10.21037/qims-22-966/rc

Conflicts of Interest: All authors have completed the ICMJE uniform disclosure form (available at https://qims.amegroups.com/article/view/10.21037/qims-22-966/coif).

The authors have no conflicts of interest to declare.

Ethical Statement: The authors are accountable for all aspects of the work in ensuring that questions related to the accuracy or integrity of any part of the work are appropriately investigated and resolved. This study was conducted in accordance with the Declaration of Helsinki (as revised in 2013). The study was approved by the institutional review board (IRB) of Sichuan Provincial People's Hospital and obtained written informed consent was provided by each female participant.

References

1. Jauniaux E, Jurkovic D. Placenta accreta: pathogenesis of a 20th century iatrogenic uterine disease. Placenta 2012;33:244-51.
2. He F, Chen D. Placenta accreta: challenging diagnosis and management strategies. Chinese Journal of Practical Gynecology & Obstetrics 2016;32:315-8.
3. Wang X, Zhao F, Li Y, Ning G, Wang X. Interpretation of Society of Abdominal Radiology and European Society of Urogenital Radiology Joint Consensus Statement for MRI imaging of Placenta Accreta Spectrum Disorders. Chin J Obstet Gynecol Pediatr (Electron Ed) 2020;16:161-70.
4. Carusi DA. The Placenta Accreta Spectrum: Epidemiology and Risk Factors. Clin Obstet Gynecol 2018;61:733-42.
5. Silver RM. Abnormal Placentation: Placenta Previa, Vasa Previa, and Placenta Accreta. Obstet Gynecol 2015;126:654-68.
6. Eller AG, Porter TF, Soisson P, Silver RM. Optimal management strategies for placenta accreta. BJOG 2009;116:648-54.
7. Warshak CR, Ramos GA, Eskander R, Benirschke K, Saenz CC, Kelly TF, Moore TR, Resnik R. Effect of predelivery diagnosis in 99 consecutive cases of placenta accreta. Obstet Gynecol 2010;115:65-9.
8. Belfort MA. Placenta accreta. Am J Obstet Gynecol 2010;203:430-9.
9. Silver RM, Landon MB, Rouse DJ, Leveno KJ, Spong CY, Thom EA, et al. Maternal morbidity associated with multiple repeat cesarean deliveries. Obstet Gynecol 2006;107:1226-32.
10. Bailit JL, Grobman WA, Rice MM, Reddy UM, Wapner RJ, Varner MW, Leveno KJ, Iams JD, Tita ATN, Saade G, Rouse DJ, Blackwell SC; . Morbidly adherent placenta treatments and outcomes. Obstet Gynecol 2015;125:683-9.
11. Belfort MA. Placenta accreta. Am J Obstet Gynecol 2010;203:430-9.
12. Eller AG, Porter TF, Soisson P, Silver RM. Optimal management strategies for placenta accreta. BJOG 2009;116:648-54.
13. Warshak CR, Ramos GA, Eskander R, Benirschke K, Saenz CC, Kelly TF, Moore TR, Resnik R. Effect of predelivery diagnosis in 99 consecutive cases of placenta accreta. Obstet Gynecol 2010;115:65-9.
14. Shamshirsaz AA, Fox KA, Salmanian B, Diaz-Arrastia CR, Lee W, Baker BW, et al. Maternal morbidity in patients with morbidly adherent placenta treated with and without a standardized multidisciplinary approach. Am J Obstet Gynecol 2015;212:218.e1-9.
15. Collins SL, Alemdar B, van Beekhuizen HJ, Bertholdt C, Braun T, Calda P, et al. Evidence-based guidelines for the management of abnormally invasive placenta: recommendations from the International Society for Abnormally Invasive Placenta. Am J Obstet Gynecol 2019;220:511-26.
16. Palacios-Jaraquemada JM, Fiorillo A, Hamer J, Martínez M, Bruno C. Placenta accreta spectrum: a hysterectomy can be prevented in almost 80% of cases using a resective-reconstructive technique. J Matern Fetal Neonatal Med 2022;35:275-82.
17. Jensen JH, Helpern JA, Ramani A, Lu H, Kaczynski K. Diffusional kurtosis imaging: the quantification of non-gaussian water diffusion by means of magnetic resonance imaging. Magn Reson Med 2005;53:1432-40.
18. Lu T, Wang Y, Guo A, Cui W, Chen Y, Wang S, Wang G. Monoexponential, biexponential and diffusion kurtosis MR imaging models: quantitative biomarkers in the diagnosis of placenta accreta spectrum disorders. BMC Pregnancy Childbirth 2022;22:349.
19. Lu T, Wang Y, Deng Y, Wu C, Li X, Wang G. Diffusion and perfusion MRI parameters in the evaluation of placenta accreta spectrum disorders in patients with placenta previa. MAGMA 2022;35:1009-20.

20. Yang M, Yan Y, Wang H. IMAge/enGINE: a freely available software for rapid computation of high-dimensional quantification. Quant Imaging Med Surg 2019;9:210-8.
21. Xiao Z, Zhong Y, Tang Z, Qiang J, Qian W, Wang R, Wang J, Wu L, Tang W, Zhang Z. Standard diffusion-weighted, diffusion kurtosis and intravoxel incoherent motion MR imaging of sinonasal malignancies: correlations with Ki-67 proliferation status. Eur Radiol 2018;28:2923-33.
22. Cui Y, Yang X, Du X, Zhuo Z, Xin L, Cheng X. Whole-tumour diffusion kurtosis MR imaging histogram analysis of rectal adenocarcinoma: Correlation with clinical pathologic prognostic factors. Eur Radiol 2018;28:1485-94.
23. Ding Y, Tan Q, Mao W, Dai C, Hu X, Hou J, Zeng M, Zhou J. Differentiating between malignant and benign renal tumors: do IVIM and diffusion kurtosis imaging perform better than DWI? Eur Radiol 2019;29:6930-9.
24. Wan Q, Deng YS, Lei Q, Bao YY, Wang YZ, Zhou JX, Zou Q, Li XC. Differentiating between malignant and benign solid solitary pulmonary lesions: are intravoxel incoherent motion and diffusion kurtosis imaging superior to conventional diffusion-weighted imaging? Eur Radiol 2019;29:1607-15.
25. Chantraine F, Blacher S, Berndt S, Palacios-Jaraquemada J, Sarioglu N, Nisolle M, Braun T, Munaut C, Foidart JM. Abnormal vascular architecture at the placental-maternal interface in placenta increta. Am J Obstet Gynecol 2012;207:188.e1-9.
26. Tantbirojn P, Crum CP, Parast MM. Pathophysiology of placenta creta: the role of decidua and extravillous trophoblast. Placenta 2008;29:639-45.
27. Moore RJ, Strachan BK, Tyler DJ, Duncan KR, Baker PN, Worthington BS, Johnson IR, Gowland PA. In utero perfusing fraction maps in normal and growth restricted pregnancy measured using IVIM echo-planar MRI. Placenta 2000;21:726-32.
28. Moore RJ, Issa B, Tokarczuk P, Duncan KR, Boulby P, Baker PN, Bowtell RW, Worthington BS, Johnson IR, Gowland PA. In vivo intravoxel incoherent motion measurements in the human placenta using echo-planar imaging at 0.5 T. Magn Reson Med 2000;43:295-302.
29. Jensen JH, Helpern JA, Ramani A, Lu H, Kaczynski K. Diffusional kurtosis imaging: the quantification of non-gaussian water diffusion by means of magnetic resonance imaging. Magn Reson Med 2005;53:1432-40.
30. Jauniaux E, Burton GJ. Pathophysiology of Placenta Accreta Spectrum Disorders: A Review of Current Findings. Clin Obstet Gynecol 2018;61:743-54.
31. Le Bihan D, Turner R. The capillary network: a link between IVIM and classical perfusion. Magn Reson Med 1992;27:171-8.
32. Liu XL, Feng J, Huang CT, Mei YJ, Xu YK. Use of intravoxel incoherent motion MRI to assess placental perfusion in normal and Fetal Growth Restricted pregnancies on their third trimester. Placenta 2022;118:10-5.
33. Andescavage N, You W, Jacobs M, Kapse K, Quistorff J, Bulas D, Ahmadzia H, Gimovsky A, Baschat A, Limperopoulos C. Exploring in vivo placental microstructure in healthy and growth-restricted pregnancies through diffusion-weighted magnetic resonance imaging. Placenta 2020;93:113-8.
34. Kristi B A, Ditte N H, Caroline H, Marianne S, Astrid P, Jens B F, David A P, Anne S. Placental diffusion-weighted MRI in normal pregnancies and those complicated by placental dysfunction due to vascular malperfusion. Placenta 2020;91:52-8.
35. Derwig I, Lythgoe DJ, Barker GJ, Poon L, Gowland P, Yeung R, Zelaya F, Nicolaides K. Association of placental perfusion, as assessed by magnetic resonance imaging and uterine artery Doppler ultrasound, and its relationship to pregnancy outcome. Placenta 2013;34:885-91.
36. Jensen JH, Helpern JA. MRI quantification of non-Gaussian water diffusion by kurtosis analysis. NMR Biomed 2010;23:698-710.
37. Rosenkrantz AB, Padhani AR, Chenevert TL, Koh DM, De Keyzer F, Taouli B, Le Bihan D. Body diffusion kurtosis imaging: Basic principles, applications, and considerations for clinical practice. J Magn Reson Imaging 2015;42:1190-202.
38. Shamshirsaz AA, Fox KA, Salmanian B, Diaz-Arrastia CR, Lee W, Baker BW, et al. Maternal morbidity in patients with morbidly adherent placenta treated with and without a standardized multidisciplinary approach. Am J Obstet Gynecol 2015;212:218.e1-9.
39. Chen C, Liu X, Chen D, Huang S, Yan X, Liu H, Chang Q, Liang Z. A risk model to predict severe postpartum hemorrhage in patients with placenta previa: a single-center retrospective study. Ann Palliat Med 2019;8:611-21.
40. Lee JY, Ahn EH, Kang S, Moon MJ, Jung SH, Chang SW, Cho HY. Scoring model to predict massive post-partum bleeding in pregnancies with placenta previa: A retrospective cohort study. J Obstet Gynaecol Res 2018;44:54-60.

41. Chen D, Xu J, Ye P, Li M, Duan X, Zhao F, Liu X, Wang X, Peng B. Risk scoring system with MRI for intraoperative massive hemorrhage in placenta previa and accreta. J Magn Reson Imaging 2020;51:947-58.
42. Ghezzi CLA, Silva CK, Casagrande AS, Westphalen SS, Salazar CC, Vettorazzi J. Diagnostic performance of radiologists with different levels of experience in the interpretation of MRI of the placenta accreta spectrum disorder. Br J Radiol 2021;94:20210827.
43. Cao L, Chen J, Duan T, Wang M, Jiang H, Wei Y, Xia C, Zhou X, Yan X, Song B. Diffusion kurtosis imaging (DKI) of hepatocellular carcinoma: correlation with microvascular invasion and histologic grade. Quant Imaging Med Surg 2019;9:590-602.

Cite this article as: Lu T, Li M, Li H, Wang Y, Zhao X, Zhao Y, Wang N. Diffusion kurtosis and intravoxel incoherent motion in predicting postpartum hemorrhage in patients at high risk for placenta accreta spectrum disorders. Quant Imaging Med Surg 2023;13(9):5921-5933. doi: 10.21037/qims-22-966

